Journal of Innovative Optical Health Sciences
Vol. 4, No. 3 (2011) 301–307

DOI: 10.1142/S1793545811001563

MINIMIZING EXCITATION LIGHT LEAKAGE AND MAXIMIZING MEASUREMENT SENSITIVITY FOR MOLECULAR IMAGING WITH NEAR-INFRARED FLUORESCENCE

BANGHE ZHU* and EVA M. SEVICK-MURACA
Center for Molecular Imaging
The Brown Foundation Institute of Molecular Medicine
The University of Texas Health Science Center at Houston
Houston, TX 77030, USA
**Banghe.Zhu@uth.tmc.edu*

Accepted 18 April 2011

Near-infrared fluorescence (NIRF) imaging involves the separation of weak fluorescence signals from backscattered excitation light. The measurement sensitivity of current NIRF imaging systems is limited by the excitation light leakage through rejection filters. In this contribution, the authors demonstrate that the excitation light leakage can be suppressed upon using appropriate filter combination and permutations. The excitation light leakage and measurement sensitivity were assessed and compared in this study by computing the transmission ratios of excitation to emission light collected and the signal-to-noise ratios in well-controlled phantom studies with different filter combinations and permutations. Using appropriate filter combinations and permutations, we observe as much as two orders of magnitude reduction in the transmission ratio and higher signal-to-noise ratio.

Keywords: Molecular imaging; fluorescence; optical filter; excitation light leakage; noise floor.

1. Introduction

In preclinical studies, near-infrared fluorescence (NIRF) imaging has demonstrated great potential for molecular imaging applications ranging from the detection of early or metastatic cancer, assessment of cancer status of sentinel lymph nodes, and staging of several other diseases. Clinically, the first applications of NIRF imaging has been limited to nonspecific indocyanine green (ICG) as the imaging agent.[1] Used safely in humans for over 50 years on the basis of its dark-green color, ICG is a poor fluorophore and has no functional groups for conjugating to targeting moieties such as peptides or antibody-based proteins. The future of NIRF molecular imaging depends upon the administration of a "first-in-humans" imaging agent that can (i) target disease markers found in tissues at pico- to femto-molar concentrations as well as (ii) provide greater fluorescent yield than ICG. Although other fluorescent molecules, such as fluorescein, have been used diagnostically in humans, their use for noninvasive, molecular imaging is limited by high autofluorescence at the visible and red excitation wavelengths (< 750 nm) as well as by limited tissue penetration

depth. NIRF imaging takes advantage of the wavelength range of 750−900 nm, where (i) the major tissue chromophores such as hemoglobin, lipid, and water exhibit their lowest absorption coefficients; (ii) NIR excitation and fluorescent light can penetrate several centimeters of tissues; and (iii) there is little or no autofluorescence to confound and lower sensitivity. The latter is especially important because unlike fluorophores excited in the visible or red wavelength ranges, there is no need for spectral unmixing to reduce autofluorescence and increase sensitivity.

However, the sensitivity of noninvasive NIRF measurements requires the separation of weak signals emanating from pico- to femto-molar tissue concentrations of targeted fluorophore from an overwhelmingly large component of scattered excitation light.[2−4] For example, in the case of micromolar tissue concentration of ICG, the re-emitted emission fluence is two orders magnitude less than the diffusely propagated excitation light that propagates to the tissue surface. If the tissue contains nanomolar quantities of ICG, then the re-emitted fluence may correspond to five orders of magnitude less than the diffusely propagated excitation light propagating to the same point.[4] If proper filtering of excitation light is not achieved, then it is impossible to detect pico- to femto-molar quantities of tissue-targeted fluorophores. Indeed, the sensitivity of NIRF is limited by the high noise floor that arises due to the excitation light leakage through band-pass and band-rejection interference filters that have been employed extensively in NIRF imaging studies without much consideration of the physics. For example, the published claims in high-impact journals that one can detect pico- to femto-molar concentrations in small animal studies using a rejection filter with optical density (OD) of two simply defies optical physics. The missing key to NIRF molecular imaging depends upon improving sensitivity by reducing the "noise" floor through proper excitation light rejection, an area of little attention.

In this contribution, the authors demonstrate that different filter combinations can significantly reduce excitation light leakage and maximize measurement sensitivity. Two phantom models were made for evaluation of instrument excitation light rejection performance and measurement sensitivity. The concepts, approach, and results presented herein are directly applicable to both preclinical and clinical fluorescence imaging systems.

2. Approach and Methods

2.1. *Image-intensified charge-coupled device−based NIRF imaging systems with different filter combinations*

An image-intensified charge-coupled device (ICCD)−based NIRF imaging system[5] used for clinical imaging of human lymphatic function[6] was modified by adding different filter combinations. First, a 785-nm laser diode outfitted with and without a 785-nm band pass "clean-up" filter (LD01−785/10, optical density >5: 705−765 nm and 803−885 nm, Semrock, Inc.) was expanded to illuminate the phantom or tissue surface uniformly through an optical diffuser and a convex lens. Fluorescent signals were collected using different filter combinations and permutation, as shown in Fig. 1. In design 1 [Fig. 1(a)] and design 2 [Fig. 1(b)], two stacked filters, one a 785-nm notch filter (HSPF785.0-1.0, optical density >6.0 at 785 nm, Kaiser Optical System, Ann Arbor, MI, USA) and the other, a 830-nm band pass filter (830FS10, optical density >5 at 785 nm, Andover, Salem, NH, USA), were placed in front of Nikon focus lens (AF NIKKOR 28 mm f/2.8D, Nikon, NY, USA). In design 3 [Fig. 1(c)], the 785-nm notch filter in the design 2 was replaced with an 830-nm band pass filter. In design 4 [Fig. 1(d)], the two 830-nm band pass filters in design 3 were separated by the Nikon focus lens. In all cases, the filtered fluorescence signals were magnified by the NIR sensitive intensifier and recorded with a 16-bit customized CCD camera (Photometrics, Tucson, AZm, USA). The whole imaging process was implemented under control of LabVIEW based interface (National Instruments, Austin, TX, USA).

2.2. *Transmission ratio for excitation light leakage*

To investigate the efficiency of the filter configurations for blocking backscattered excitation light and collecting propagated fluorescence signals, a liquid phantom of 2 L of 1.0% Liposyn scattering solution in a cylindrical container was employed. Excitation light leakage was defined as the signal $S(\lambda_x)$, or average pixel intensity values over a region of interest (ROI) of the scattering surface taken without ICG in solution. The fluorescence signal along with possible contamination from excitation light, $S(\lambda_m + \lambda_x)$, was likewise averaged

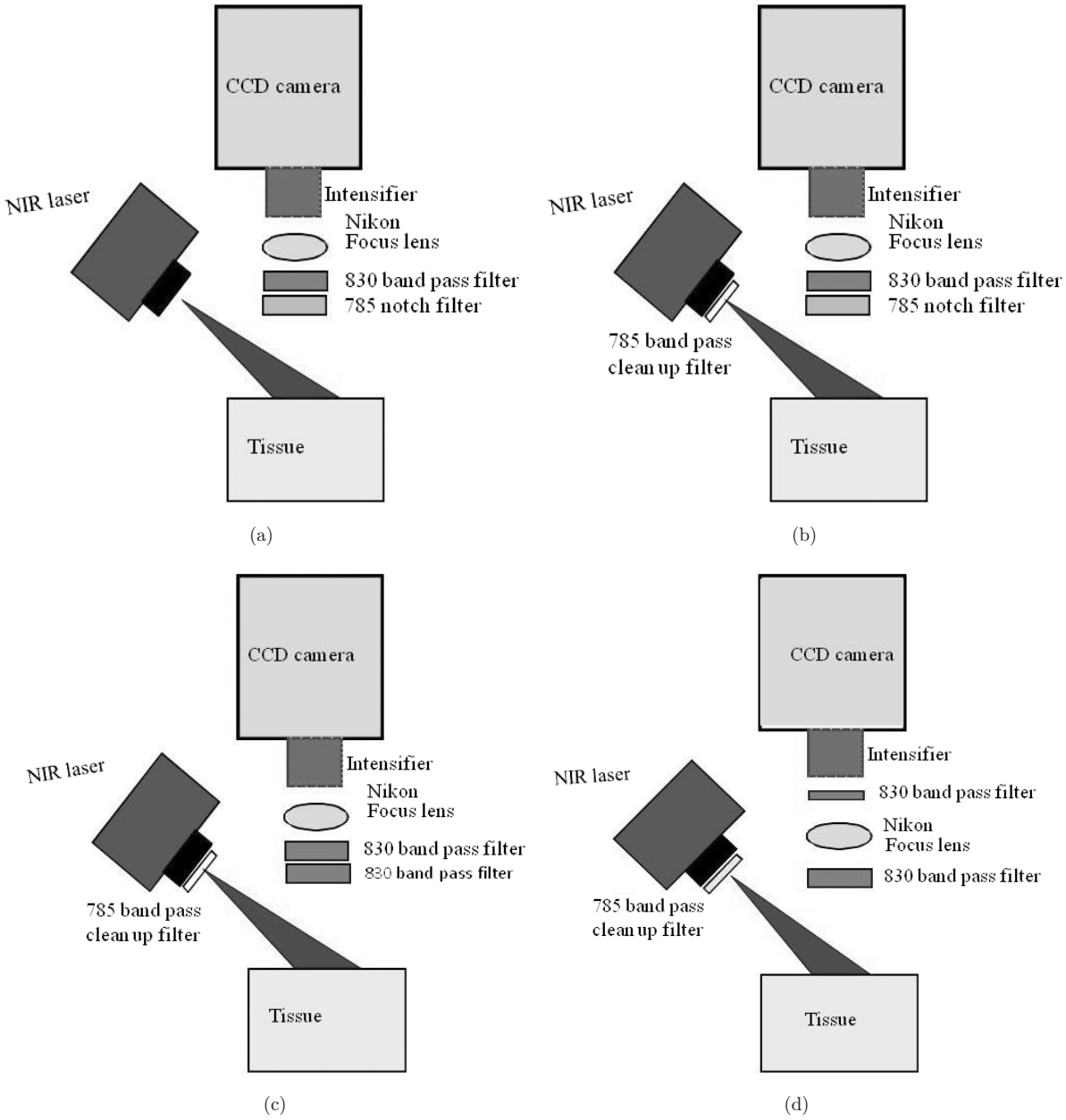

Fig. 1. Schematic of design 1 (a); design 2 (b); design 3 (c) and design 4 (d) of ICCD-based NIRF imaging system.

from the pixel intensity values over the same ROI taken after adding ICG to constitute a 1.0-nM solution. For different filtering designs, the signal was integrated to achieve maximum counts of signal, $S(\lambda_m + \lambda_x)$ on the CCD camera of around 40,000. Typically, this required between 200 and 900 ms. For each individual design, the ICCD integration time, intensifier gain, and laser power (<1.9mW/cm^2) were maintained constant for collection of $S(\lambda_x)$ and $S(\lambda_m + \lambda_x)$ signal. Other system effects that may add to noise level were typically removed through an additional subtraction of the mean ambient noise (obtained without laser excitation light) from measurements. The transmission ratio R was then calculated using the following equation[2–4]:

$$R = \frac{S(\lambda_x)}{S(\lambda_m + \lambda_x) - S(\lambda_x)}, \tag{1}$$

where $S(\lambda_x)$ signals can be called as the "off-band" transmission signals, whereas the differences, signal $S(\lambda_m + \lambda_x) - S(\lambda_x)$, represent the "in-band" transmission signals.

2.3. *Signal-to-noise ratio*

To evaluate fluorescence imaging instrument sensitivity, the signal-to-noise ratio (SNR) of various designs of NIRF imaging system was measured on a fluorescent mouse-shaped phantom (Caliper, Hopkinton, MA, USA). The mouse-shaped phantom is made of polyurethane material that includes scattering particles and dye to simulate the optical properties of live tissue. Rods containing a fluorescent probe embedded in the tip were inserted into the phantom to simulate an internal fluorescent light source. Measurements were conducted and the SNR computed:

$$\mathrm{SNR} = 20\mathrm{Log10}\left(\frac{F_{\mathrm{counts}}}{N_{\mathrm{counts}}}\right), \tag{2}$$

where F_{counts} is the average pixel counts of the difference between the fluorescence signals and the control (blank rod inserted) over the ROI containing the inserted rod tip. N_{counts} represents the average pixel count of signals taken from the same ROI in the absence of fluorophores in the rod. For different filter combinations, we varied the CCD integration time to achieve around 40,000 counts when the fluorescent inclusion was used. Again, measurement settings such as the intensifier gain, CCD camera integration time, and laser power were held constant when data for fluorescent and non-fluorescent inclusions were taken.

3. Results

Transmission ratio for excitation light leakage: Fig. 2 presents the calculated transmission ratio and integration time versus various filter configurations of the NIRF imaging system. As shown, the magnitude of transmission ratio decreases approximately five times by using the "clean up" filter (comparing design 1 and 2 in Fig. 1). By substituting 830-nm band pass filter for 785 nm notch filter, the transmission ratio decreases further (comparing design 2 to 3). When the two 830-nm band pass filters are separated by the Nikon focus lens, the magnitude of transmission ratio decreases as much as 7.5 times (comparing design 3 to 4). Overall, we observe as much as two orders of magnitude reduction in the ratio of off-band to in-band transmission using design 4 compared to design 1. The integration time is variable for different designs, but it is still within the acceptable range for clinical application.

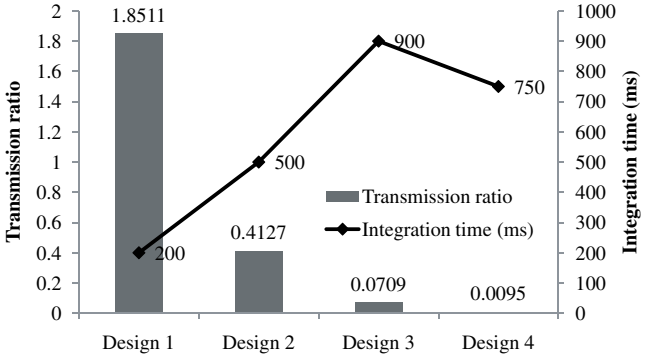

Fig. 2. Transmission ratio and integration time of NIRF imaging for various designs.

SNR: From visual comparison of Figs. 3(a)–3(d), one can see that fluorescence signals are contaminated by different levels of noise. The calculated SNR shown in Fig. 4 demonstrates the greatest measurement sensitivity of NIRF imaging obtained using design 4. For the design 1, the calculated SNR is negative, indicating the fluorescence signals are lower than noise and in this case no meaningful information should be obtained. These results also indicate that excitation light leakage makes a considerable contribution to the noise floor.

4. Discussion

The performance of the ICCD-based NIRF imaging system is primarily influenced by the shot noise[7] and the leakage of ambient and excitation light through optical filters.[4] This is because readout and dark current noise are negligible. However, shot noise is caused by the statistical fluctuations of detected photons, which are always present in imaging systems. Hence, the excitation light leakage currently represents the limiting noise floor of NIRF imaging systems. The excitation light leakage in fluorescence imaging may arise from one or more of the following: (i) laser diodes have side-band components located at emission wavelength of NIR dyes; (ii) the "blue shift" phenomenon of optical filters as the incident light deviates from normal incidence; and (iii) the optical filters have the limited OD.

Typically, laser diode output is considered monochromatic and its spectra described by a prominent line corresponding to a single output wavelength. However, there often exist side-band components or second peaks due to lower level

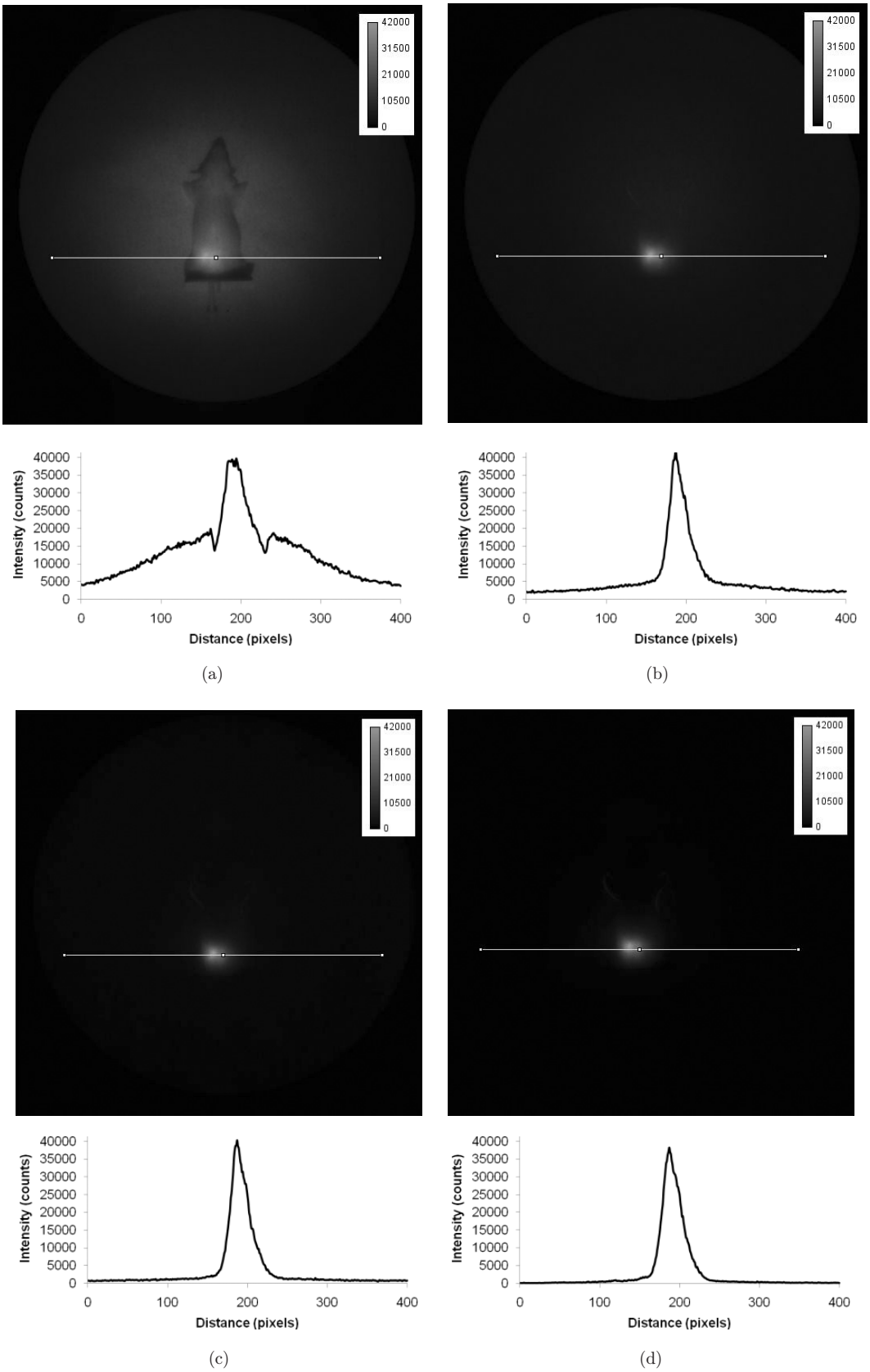

Fig. 3. Images and profiles of a line drawn across the portion of images which contained the inserted rod tip of fluorescence mouse-shaped phantom using design 1 (a), design 2 (b), design 3 (c), and design 4 (d), respectively.

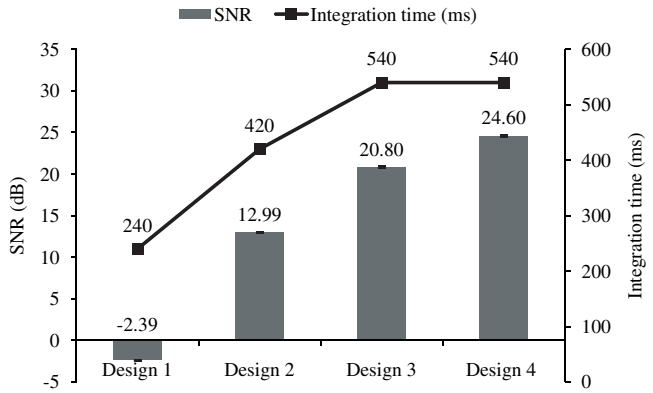

Fig. 4. Signal-to-noise ratio and integration time versus various designs of NIRF imaging system.

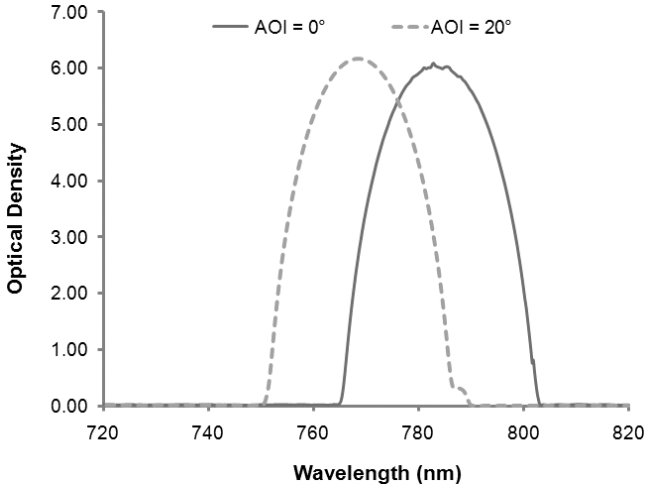

Fig. 5. Optical density of 785-nm notch filter at two different incident angles, where AOI represents the angle of incidence.

transitions, plasma, and "glows" — all of which can be located at the emission wavelength of near-infrared dyes. Hence, introduction of "clean-up" filter may attenuate any undesirable side-band components, resulting in the reduction of excitation light leakage, as shown in design 2.

The spatial distribution of excitation light is influenced by uniformity of illumination source and illumination angle, both of which play an important role in the fluorescence imaging. If the illumination intensity varies across the field-of-view, the fluorescence image needs to be normalized by a reference illumination image. In our design, a diffuser was used to illuminate the phantom surface uniformly. In general, optical interference filters are designed to filter collimated light at a small tolerance from the angle of normal incidence. An increase in the incident angle causes a shift in maximal spectral performance toward shorter wavelengths, called the "blue shift".[3] For example, a 785-nm notch filter becomes a 765-nm notch filter at a 20° angle of incidence shown in Fig. 5 as computed from data provided by Semrock Inc. Under these conditions, the filter passes instead of blocking 785-nm backscattered excitation light. In comparison, the 830-nm band pass filter has larger tolerance from the incident angles in blocking 785-nm backscattered excitation light, as demonstrated in design 3.

To separate the weak fluorescence signals from the overwhelmingly larger component of scattered excitation light, one or several filter combinations are generally used to obtain higher optical density (OD) at the excitation wavelength. However, the combined OD is not the direct sum of each filter OD. This is because of cancellations due to multiple-path interference between two filters occurs. However, a small amount of loss inserted between two filters can efficiently cancel the multiple-path interference effects and increase the combined OD. In design 4, the Nikon focus lens and aperture act as loss materials, which largely increase the combined OD, and reduce the excitation light leakage.

In conclusion, the excitation light leakage in the ICCD-based NIRF imaging system can be reduced dramatically by use of the appropriate filter combinations and permutations as performed in design 4. The calculated SNR indicates that excitation light leakage makes a considerable contribution to the noise floor. The parameter of transmission ratio R should be used as a quantifiable metric for manufacturers of instrumentation for investigators who need to report operation qualifications to enable comparison of their results. The approach for reduction of excitation light leakage in the ICCD-based NIRF imaging system should be extended to all fluorescence enhanced optical imaging systems which can potentially suffer from high "noise floor." Indeed, before time-dependent techniques (such as time- and frequency-domain approaches) which can dramatically reduce instrument function are employed for NIRF tomography, instrument sensitivity needs to be maximized.

Finally, if clinical NIRF molecular imaging is to be efficiently realized, then the risks associated with "first-in-humans" NIRF imaging agents needs to be minimized and the benefits for detecting disease markers at pico- to femto-molar tissue concentrations

need to be maximized. To minimize risk, we need to administer lower doses of imaging agent. To maximize benefit of a low dose of NIR contrast agent, we need to optimize measurement sensitivity to enable detection of pico- to femto-molar quantities of "first-in-humans" imaging agents. Both are achieved by decreasing the noise floor and increasing the sensitivity of NIRF instrumentation.

Acknowledgments

This research is supported by the National Institutes of Health, R01 CA112679 and U54 CA136404 and the Texas Star Award.

References

1. M. V. Marshall, J. C. Rasmussen, I. C. Tan, M. B. Aldrich, K. E. Adams, X. Wang, C. E. Fife, E. A. Maus, L. A. Smith, E. M. Sevick-Muraca, "Near-infrared fluorescence imaging in humans with indocyanine green: A review and update," *Open Surg. Oncol. J.* **2**, 12−25 (2010).
2. J. P. Houston, A. B. Thompson, M. Gurfinkel, E. M. Sevick-Muraca, "Sensitivity and depth penetration of continuous wave versus frequency-domain photon migration near-infrared fluorescence contrast-enhanced imaging," *Photochem. Photobiol.* **77**, 420−430 (2003).
3. K. Hwang, J. P. Houston, J. C. Rasmussen, A. Joshi, S. Ke, C. Li, E. M. Sevick-Muraca, "Improved excitation light rejection enhances small-animal fluorescent optical imaging," *Mol. Imaging* **4**, 194−204 (2005).
4. B. Zhu, J. C. Rasmussen, Y. Lu, E. M. Sevick-Muraca, "Reduction of excitation light leakage to improve near-infrared fluorescence imaging for tissue surface and deep tissue imaging," *Med. Phys.* **37**, 5961−5970 (2010).
5. J. S. Reynolds, T. L. Troy, E. M. Sevick-Muraca, "Multipixel techniques for frequency domain photon migration imaging," *Biotechnol. Prog.* **13**, 669−680 (1997).
6. J. C. Rasmussen, I. Tan, M. V. Marshall, C. E. Eife, E. M. Sevick-Muraca, "Lymphatic imaging in humans with near-infrared fluorescence," *Curr. Opin. Biotechnol.* **20**, 74−82 (2009).
7. D. Dussault, P. Hoess, "Noise performance comparison of ICCD with CCD and EMCCD cameras," *Proc. SPIE* **5563**, 195−204 (2004).